arXiv:1510.03460v1 [hep-ph] 12 Oct 2015

# Towards the Final Word on Neutralino Dark Matter

Joseph Bramante,[1] Nishita Desai,[2] Patrick Fox,[3]
Adam Martin,[1] Bryan Ostdiek,[1,4] and Tilman Plehn[2]

[1] *Department of Physics, University of Notre Dame, IN, USA*
[2] *Institut für Theoretische Physik, Universität Heidelberg, Germany*
[3] *Theoretical Physics Department, Fermilab, Batavia, IL USA*
[4] *Department of Physics, University of Oregon, OR, USA*

We present a complete phenomenological prospectus for thermal relic neutralinos. Including Sommerfeld enhancements to relic abundance and halo annihilation calculations, we obtain direct, indirect, and collider discovery prospects for all neutralinos with mass parameters $M_1, M_2, |\mu| < 4$ TeV, that freeze out to the observed dark matter abundance, with scalar superpartners decoupled. Much of the relic neutralino sector will be uncovered by the direct detection experiments Xenon1T and LZ, as well as indirect detection with CTA. We emphasize that thermal relic higgsinos will be found by next-generation direct detection experiments, so long as $M_{1,2} < 4$ TeV. Charged tracks at a 100 TeV hadron collider complement indirect searches for relic winos. Thermal relic bino-winos still evade all planned experiments, including disappearing charged-track searches. However, they can be discovered by compressed electroweakino searches at a 100 TeV collider, completing the full coverage of the relic neutralino surface.

## CONTENTS

I. Introduction 2

II. Sommerfelded Relic Neutralino Surface 3

III. Direct Detection 6

IV. Indirect Detection 8

V. 100 TeV Collider 10
A. Charged track search 11
B. Compressed search 13

VI. Conclusions 14

Acknowledgments 15

References 15

## I. INTRODUCTION

While it is sometimes claimed that no physics beyond the Standard Model need appear below energy scales accessible to imminent experiments, this is not true for weakly interacting, thermally produced neutralino dark matter. In the minimal supersymmetric standard model (MSSM), the primary dark matter (DM) candidate is the lightest neutralino, which is an admixture of neutral binos, winos, and higgsinos. Prior studies have considered which combination of these interaction eigenstates freeze out to the observed relic abundance. Starting from these pure states, the relic neutralino surface [1] is limited by abundance criteria to TeV-scale particle masses, which means that dark matter could be unmasked at ongoing direct detection, collider, and indirect detection experiments [2–52].

In this work, we advance these phenomenological efforts by including the Sommerfeld enhancement to thermal freeze-out annihilation for the relic neutralino surface, *i.e.* $M_1, M_2, |\mu| \lesssim 4$ TeV. This enhancement substantially alters neutralino masses and experimental prospects whenever $M_2 \gtrsim 1$ TeV, a region which has often been omitted in prior work. In addition, we clarify some facets of relic neutralino phenomenology:

- It is sometimes stated that future direct detection experiments will cover most MSSM neutralino parameter space. We find that a preponderance of relic bino-wino parameter space ($M_2 \sim M_1 \simeq 0.2 - 2$ TeV and $|\mu| \gtrsim 2$ TeV) cannot be probed by direct, indirect, or LHC searches. The reason is that the lightest supersymmetric partner (LSP) contains only tiny higgsino and wino fractions, so its annihilation cross-section, along with spin-independent and spin-dependent scattering on nucleons are suppressed. In addition, the GeV-level bino-wino mass splitting between the lightest chargino (CLSP) and the LSP renders collider charged-track searches ineffective.

- As authors of this paper explored in prior work, the relic bino-wino region can be uncovered with compressed electroweakino searches at a 100 TeV proton-proton collider [1]. We refine these findings for the Sommerfeld-enhanced relic neutralino surface in Section V.

- The well-known systematic uncertainty in the Milky Way's dark matter halo density profile obfuscates whether gamma ray searches can exclude, have excluded, or will exclude $M_2 \gtrsim 2$ TeV thermal relic neutralinos. However, future charged track searches at a 100 TeV proton-proton collider will be most sensitive to this wino-like LSP parameter space where gamma ray constraints are weakest, namely when $|\mu| \sim 4$ TeV and $M_1 \sim 2 - 4$ TeV.

- Contrary to the common lore that higgsino dark matter is un-discoverable, we point out that higgsinos that freeze out to the observed dark matter relic abundance ($m_{\tilde{H}} \sim 1.1$ TeV) will be discovered by next-generation direct detection experiments so long as $M_{1,2} \lesssim 4$ TeV.

Generally, we find that forthcoming experimental endeavors will be able to probe the entire relic neutralino surface for $M_1, M_2, |\mu| \lesssim 4$ TeV. Thus it seems that any "weak scale" MSSM neutralino sector can be conclusively tested out in the coming decades [1, 53–55].

In the remaining sections of this paper, we will explore present and future experimental probes of MSSM dark matter across the Sommerfeld-enhanced relic neutralino surface. In each section, we show how neutralino phenomenology across the surface can be related to either some element of the neutralino and chargino mixing matrices, or a mass splitting between electroweakino mass eigenstates. Along the way, we indicate to what extent Sommerfeld-enhanced thermal freeze-out alters neutralino phenomenology.

In Section II we introduce the Sommerfeld-enhanced relic neutralino surface, noting that the parameter space boundary where the Sommerfeld effect becomes substantial (>TeV mass neutralinos) can be understood as a consequence of the wino fraction of the LSP, the tree-level wino annihilation cross-section, and the LSP's freeze-out temperature compared to the mass of the W and Z bosons [56]. In Section III we show spin-independent and spin-dependent direct detection prospects, which are determined by the higgsino and wino fractions of the LSP, respectively [53]. In Section IV, we display the present and future reach of searches for neutralinos annihilating to gamma rays in the galactic center, which depends upon the wino fraction of the LSP. Section V presents charged track and compressed $\gamma, \ell, \not{p}_T$ searches at a 100 TeV collider across the relic neutralino surface. The charged track search depends on the mass splitting between the charged lightest supersymmetric partner (CLSP) and the LSP, while the the mass splitting between the LSP and the next to lightest neutral supersymmetric partner (NLSP) determines the efficacy of the compressed search. In Section VI we conclude.

## II. SOMMERFELDED RELIC NEUTRALINO SURFACE

This section introduces the sommerfelded* relic neutralino surface and shows that wino-like LSPs will have enlarged freeze-out annihilation from Sommerfeld-enhancement (SE)[57]. Hereafter, we will focus on neutralinos in the MSSM, with all scalar superpartners decoupled. In our numeric calculations with `SuSpect`, `microMEGAs`, `DarkSUSY`, `MG5aMC@NLO`, and `DarkSE` we fix all scalar masses to 8 TeV, including that of the CP odd Higgs. For 100 TeV proton-proton collider studies, in which $t$-channel squark exchange with a squark mass of 8 TeV can substantially increase neutralino production, we remove sfermions entirely. For the whole set of neutralino and chargino detection processes, decoupled squarks present a worst-case scenario, whereas for specific mixed scenarios, the $s$-channel and $t$-channel contributions can almost entirely cancel each other. Heavy

* From *to sommerfeld*, *i.e.* enhance through a Sommerfeld factor [57]. Another possibility would be *sommerfelled* relic neutralino surface, but in spite of the better sound to it we find that this version might be less clear.

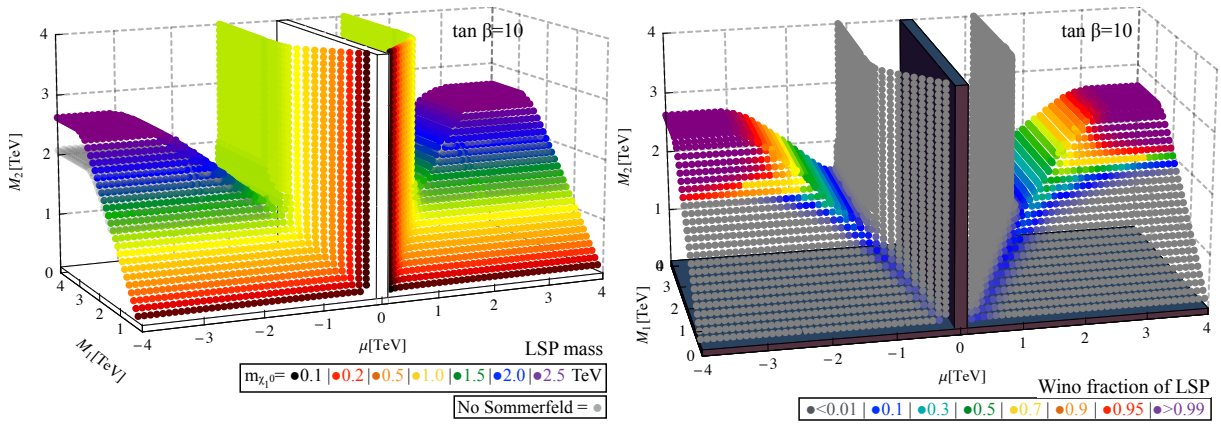


Figure 1. **Left panel:** Combinations of neutralino mass parameters $M_1, M_2, \mu$ that produce the correct relic abundance, accounting for Sommerfeld-enhancement, along with the LSP mass. The relic surface without Sommerfeld enhancement is underlain in gray. Regions excluded by LEP are occluded with a white box. **Right panel:** The wino fraction of the lightest neutralino.

sfermions are also motivated by models of split supersymmetry, where most scalar supersymmetric partners are decoupled [58–71].

Neutralinos in the MSSM are mixtures of the spin-$\frac{1}{2}$ superpartners of the weak gauge bosons, hypercharge gauge bosons, and Higgs bosons. After electroweak symmetry is broken, the neutral and charged states mix to form neutralinos and charginos, respectively. We identify the neutralinos as $\tilde{\chi}_i^0 = N_{ij}(\tilde{B}, \tilde{W}^0, \tilde{H}_u^0, \tilde{H}_d^0)$ and the charginos as $\tilde{\chi}_i^\pm = V_{ij}(\tilde{W}^\pm, \tilde{H}^\pm)$. Here $\tilde{B}, \tilde{W}, \tilde{H}_d^0, \tilde{H}_u^0$, are the bino, wino, and higgsino fields; $N_{ij}$ and $V_{ij}$ are the neutralino and chargino mixing matrices in the bino-wino basis, such that $i$ and $j$ index mass and gauge respectively [72]. The bino, wino, and higgsino mass parameters are $M_1$, $M_2$, and $\mu$, and $\tan\beta$ defines the ratio of up- and down-type Higgs boson vacuum expectation values in the MSSM.

Assuming that all scalar superpartners are heavy, when the universe cools to $T_{\rm rad} <$ TeV during radiation dominated expansion, MSSM neutralinos freeze out to a relic abundance determined by their rate of annihilation to Standard Model particles. For neutralinos with masses below 1 TeV, it is often sufficient to use tree-level annihilation cross-sections and ignore the initial state exchange of photons and weak bosons between annihilating neutralinos. On the other hand, the exchange of gauge bosons between two initial-state particles can substantially alter the annihilation probability of neutralinos with masses above 1 TeV. At threshold this higher-order correction can diverge like $1/v$, where $v$ is the relative velocity of the two incoming states. For a Yukawa-like potential, mediated for example by a $Z$-boson, this effect is cut off at $v \approx m_Z/m_{\tilde{\chi}}$, leading to large effects for a large ratio of LSP vs weak boson masses. This non-relativistic modification of the potential of two incoming states is called the Sommerfeld effect. For freeze-out temperatures below the mass of electroweak bosons ($T_{\text{freeze-out}} \equiv m_{\tilde{\chi}}/20 \lesssim 0.1$ TeV), and thus for lighter LSPs, the contribution of $W^\pm$ exchange to the effective potential of neutralino pairs is suppressed by factors of $e^{-m_W/T_{\rm rad}}$ [56].

To understand when the Sommerfeld enhancement will affect the freeze-out of mixed neutralinos, it is useful to first consider the thermal relic abundance of pure neutralino states. With decoupled scalars, two neutralinos or charginos can either annihilate through an $s$-channel $Z$ or Higgs boson, or through a $t$-channel neutralino or chargino. For the lightest neutralinos the relevant couplings

are

$$\begin{aligned} g_{Z\tilde{\chi}_1^0\tilde{\chi}_1^0} &= \frac{g}{2\cos\theta_w}\ \left(|N_{13}|^2 - |N_{14}|^2\right) \\ g_{h\tilde{\chi}_1^0\tilde{\chi}_1^0} &= \left(gN_{11} - g'N_{12}\right)\ \left(\sin\alpha\ N_{13} + \cos\alpha\ N_{14}\right) \\ g_{W\tilde{\chi}_1^0\tilde{\chi}_1^+} &= \frac{g\sin\theta_w}{\sqrt{2}\cos\theta_w}\ \left(N_{14}V_{12}^* - \sqrt{2}N_{12}V_{11}^*\right)\ , \end{aligned} \tag{1}$$

given in terms of the usual weak gauge couplings, the Higgs mixing angle $\alpha$, and the neutralino and chargino mixing matrices.

Obviously pure bino states do not couple to gauge or Higgs bosons, so no direct annihilation process exists, and their annihilation as well as Sommerfeld enhancement can only occur through mixing and co-annihilation.

For pure wino states we need to include the lightest chargino, typically with a sub-GeV mass difference. Following Eq.(1) there will still be no $s$-channel annihilation process, but for example the LSP can annihilate through the wino-like chargino in the $t$-channel. Because the two states are highly mass degenerate, the computation of the current relic abundance has to include a combined annihilation of the lightest neutralino and chargino. Neutralino-chargino co-annihilation proceeds through an $s$-channel $W$ exchange, while diagonal neutralino and chargino annihilation require a $t$-channel diagram. In the chargino case the exchange of electroweak bosons between the two non-relativistic incoming particles leads to a sizeable Sudakov enhancement: an increased cross section in the numerator of Eq.(2) has to be compensated by a larger wino mass on the relic neutralino surface,

$$\Omega_{\tilde{W}}h^2 \simeq 0.12\left(\frac{m_{\tilde{\chi}}}{2.1\ \text{TeV}}\right)^2 \xrightarrow{\text{SE}} 0.12\left(\frac{m_{\tilde{\chi}}}{2.6\ \text{TeV}}\right)^2\ . \tag{2}$$

In the top panel of Figure 1 this fact appears graphically — the sommerfelded surface, shown with LSP masses colored, separates from gray points calculated without Sommerfeld enhancement when $m_{\tilde{\chi}} \sim 1.5$ TeV, where the wino fraction is sizable.

Finally, pure higgsinos can annihilate efficiently through an $s$-channel $Z$ diagram. Co-annihilation within the triplet of two neutralinos and one chargino sets the relic density. The main distinction between this and the pure wino case, is that chargino pair annihilation contributes much less to the complete annihilation process. Because higgsino annihilation is generally more efficient, and because the contribution of chargino pair annihilation with a possible electroweak boson exchange between the incoming particles is suppressed, today's relic density is given by

$$\Omega_{\tilde{H}}h^2 \simeq 0.12\left(\frac{m_{\tilde{\chi}}}{1.13\ \text{TeV}}\right)^2 \xrightarrow{\text{SE}} 0.12\left(\frac{m_{\tilde{\chi}}}{1.14\ \text{TeV}}\right)^2\ . \tag{3}$$

This relatively small effect is hardly visible in Figure 1. There are two reasons why the Sommerfeld enhancement is significantly larger for the wino case: first, pure chargino co-annihilation with a photon-induced Sommerfeld effect is roughly three times more important for pure winos. Second, as previously noted, the $W, Z$-induced Sommerfeld effect is cut off at $v \approx m_{W,Z}/m_{\tilde{\chi}}$ (compare this to the freeze-out temperature, $\sim m_{\tilde{\chi}}/20$), which means that it influences more phase-space for pure winos at freeze-out.

To generate the sommerfelded surface shown in Figure 1, we first calculate electroweakino mass parameters with `SuSpect` [73]. We include the loop-level, custodial-symmetry-breaking-induced mass separation between the charged and neutral components of both the wino and higgsino, setting these to 160 MeV [74–76] and 350 MeV [77–79] respectively, before diagonalizing electroweakino

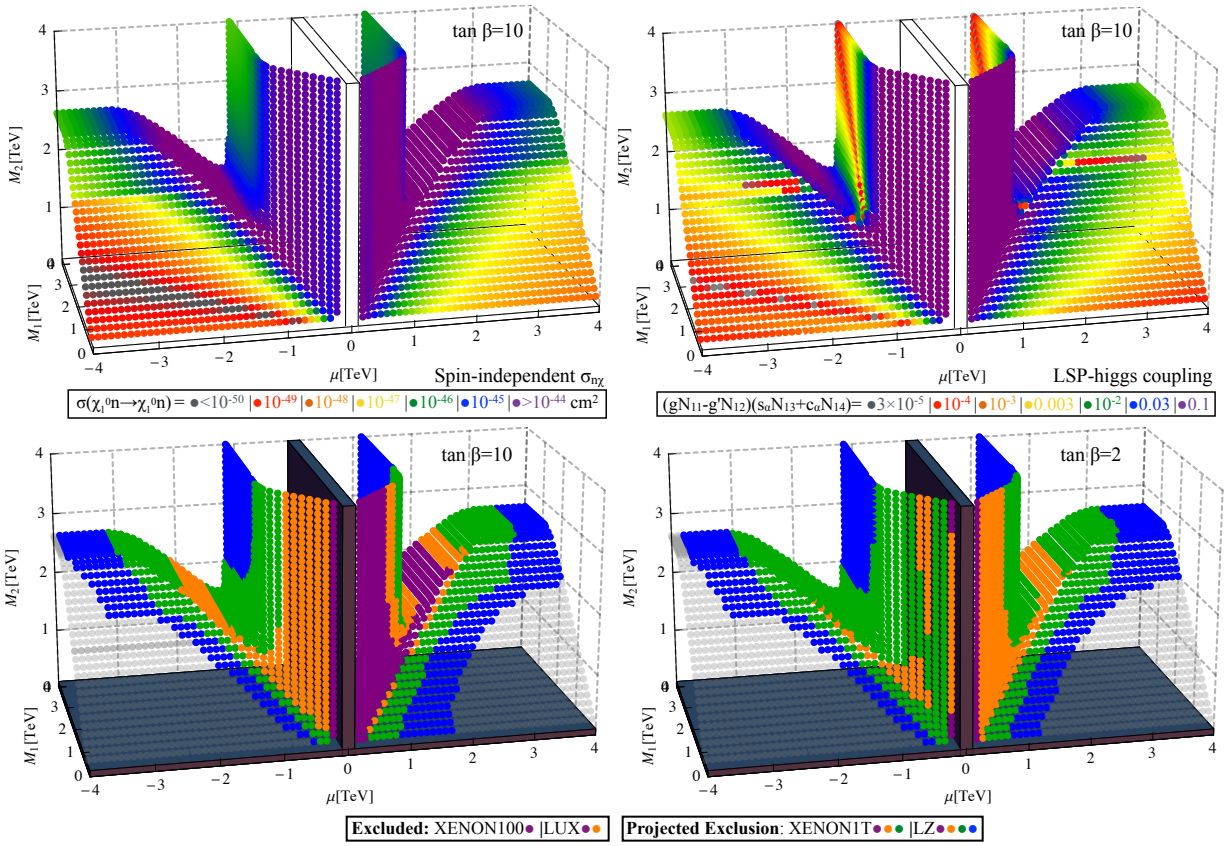


Figure 2. **Top left panel:** The spin-independent nucleon-scattering cross-section for relic neutralinos is shown, as calculated by `microMEGAs` [83]. **Top right panel:** The coupling of neutralinos to the SM-like MSSM Higgs boson. **Bottom left panel:** Relic neutralino exclusions from XENON100 and LUX and prospects from XENON1T and LZ for $\tan\beta = 10$. The boxed out area denotes the LEP exclusion. **Bottom right panel:** The same for $\tan\beta = 2$.

mass matrices. As we discuss further in Section V, the values of electroweakino mass parameters can also substantially shift these charged-neutral mass splittings. With this electroweakino mass spectrum, we require each point to satisfy $\Omega_{\tilde{\chi}} h^2 \simeq 0.12 \pm 0.005$, calculating the sommerfelded relic abundance using `DarkSE` [80, 81], which improves upon the relic density calculations of `DarkSUSY` [36], and includes Sommerfeld contributions to each LSP annihilation channel, for up to three charge-equivalent initial state pairs of electroweakinos.

As a comparison to the relic neutralino surface in Ref. [1], we also calculate the sommerfelded surface in the pure wino approximation using `microMEGAs` and following the procedure in Ref. [82]. Without Sommerfeld enhancement, the calculated relic density differs between the two programs by about 10%, with `microMEGAs` giving the higher number. After including the Sommerfeld enhancement, the maximal wino-like LSP mass from `microMEGAs` is 2.5 TeV, compared to 2.6 TeV from `DarkSE`.

## III. DIRECT DETECTION

Detection of neutralinos via nuclear scattering experiments can be divided into two categories: spin-independent (SI) and spin-dependent (SD). In the spin-independent case, neutralinos will scatter off nucleons via the exchange of a Higgs boson, which couples to quarks and quark loops

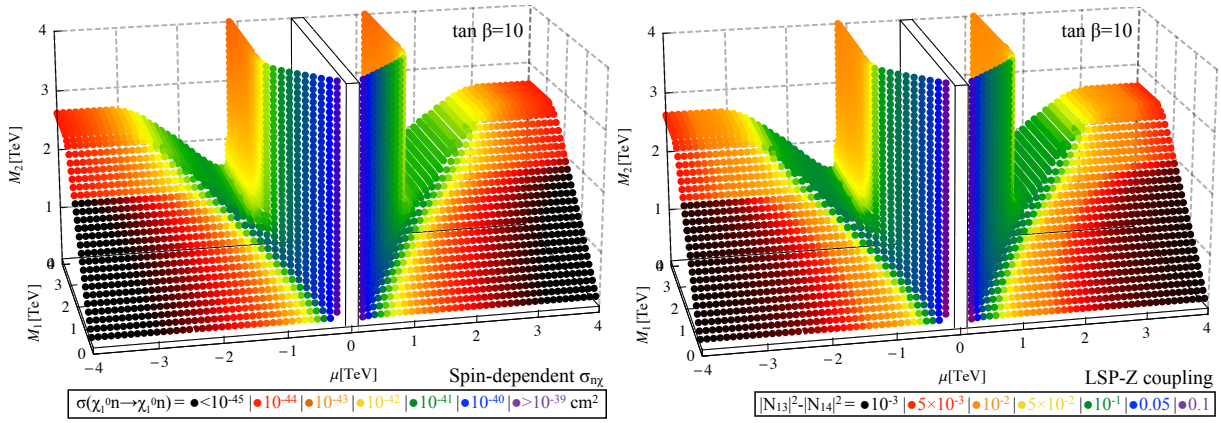


Figure 3. **Left panel:** The spin-dependent nucleon-scattering cross-section for relic neutralinos, as calculated by `microMEGAs` [83]. **Right panel:** The proportional coupling of neutralinos to the $Z$ boson.

within nucleons in atomic nuclei [28, 52, 84–87]. Following Eq.(1) this coupling is driven by bino–higgsino and wino–higgsino mixing. The spin-independent scattering will be maximized when the LSP is an even bino–higgsino or wino–higgsino mixture. Providing confirmation, Figure 2 shows that the LSP-Higgs coupling is indeed proportional to the size of SI neutralino-nucleon scattering over the relic neutralino surface — and that SI scattering cross-sections reach their apex on the bino-higgsino and wino-higgsino slopes, $M_{1,2} \sim \mu$. The apparent proportionality between coupling and scattering would be more exact if we incorporated the small but non-negligible contribution of the heavy Higgs bosons.

The SI neutralino-nucleon cross-sections in Figure 2 are obtained from `microMEGAs` [83]. The lower panels of Figure 2 also display the current exclusions on spin-independent neutralino-nucleon scattering from Xenon100 [88] and LUX [89], along with projected exclusions from Xenon1T and LZ [90]. These projections indicate that all relic neutralinos lighter than 4 TeV, except a large swathe of bino-winos (addressed in Section V), will be probed by upcoming direct detection experiments.

The cross-sections found for SI scattering here match to within a factor of two, recent studies of neutralino-nucleon scattering in a particular decoupling limit, Refs. [85–87].† Even taking $M_1 \to \infty$ or $M_2 \to \infty$ as in [85], the resulting 1.1 TeV mass higgsino appears to be within reach of LZ [90], so long as $M_2 < 4$ TeV or $M_1 < 4$ TeV.

In the case of spin-dependent scattering, which occurs through $Z$-boson exchange, and thus depends upon the spin of the nuclear scattering target, the detection of neutralinos depends solely on the higgsino fractions of the neutralino (*i.e.* what portions are $H_u, H_d$). As shown in Eq.(1), binos and winos do not couple to the $Z$ boson. Moreover, if $|N_{13}| = |N_{14}|$, which happens for pure Higgsinos, the neutralino spin-dependent scattering cross-section vanishes. In Figure 3 we show the spin-dependent neutralino-nucleon scattering cross-section, as well as the LSP-$Z$ coupling across the relic neutralino surface. The correspondence is striking — the size of the $Z$-neutralino coupling determines the size of the spin-dependent cross-section. Constraints from the current generation

† In our work, the least coupled higgsino-like LSP point shown in Figure 2 has a cross-section,

$$(M_1 = 4 \text{ TeV}, M_2 = 4 \text{ TeV}, |\mu| = 1.1 \text{ TeV}) \to \sigma^{(\text{SI})}_{n\tilde{\chi}} \simeq 10^{-46} \text{ cm}^2.$$

For this point, matching Eq. (1) to the higgs-LSP coupling of Ref. [85], and using this to determine $\kappa$ in Ref. [85] yields

$$(M_1 \to \infty, M_2 = 4 \text{ TeV}, |\mu| = 1.1 \text{ TeV}) \to \sigma^{(\text{SI})}_{n\tilde{\chi}} \simeq 7 \times 10^{-47} \text{ cm}^2$$
$$(M_1 = 4 \text{ TeV}, M_2 \to \infty, |\mu| = 1.1 \text{ TeV}) \to \sigma^{(\text{SI})}_{n\tilde{\chi}} \simeq 7 \times 10^{-47} \text{ cm}^2.$$

of spin-dependent scattering of relic neutralino dark matter at experiments like SIMPLE [91], COUPP [92], Xenon100 [93], and PICO2L [94], are less stringent than spin-independent constraints. However, future experiments like PICO250 [90] will be able to probe TeV-mass thermal relic bino-higgsinos.

## IV. INDIRECT DETECTION

Gamma ray surveys of the galactic center have bounded dark matter annihilation to photons, $\tilde{\chi}_1^0\tilde{\chi}_1^0 \to \gamma\gamma, Z\gamma$, or intermediate particles which decay to photons, $\tilde{\chi}_1^0\tilde{\chi}_1^0 \to W^+W^-$. However, these bounds remain somewhat uncertain, because they depend upon the Milky Way's DM density profile. The flux of photons $\Phi_\gamma$ arising from dark matter annihilating inside an observed cone of solid angle $\Delta\Omega$ is

$$\frac{d\Phi_\gamma}{dE_\gamma} = \frac{\langle\sigma v\rangle}{8\pi m_X^2}\,\frac{dN_\gamma}{dE_\gamma}\int_{\Delta\Omega} d\Omega \int_{\text{line of sight}} dl\ \rho_{\tilde{\chi}}^2(l)\ , \tag{4}$$

where $E_\gamma$ is the energy of the photon, $\langle\sigma v\rangle$ is the averaged DM annihilation cross-section, $N_\gamma$ is the number of photons produced per annihilation, and $l$ is the distance from the observer to the DM annihilation event.

Because Eq.(4) is proportional to $\rho_{\tilde{\chi}}^2$, any annihilation constraint relies on assumptions about the Milky Way's DM density profile. Assuming a steeper DM halo profile, *i.e.* DM density increasing more rapidly towards the core of the Milky Way, results in a more stringent bound on DM annihilation. We consider three DM halo density profiles that are increasingly flat towards the center of the Milky Way. The generalized NFW profile [95] is given by

$$\rho_{\rm NFW}(r) = \frac{\rho_\odot}{(r/R)\,(1+r/R)^2}, \tag{5}$$

where $r$ is the distance from the galactic center, and we assume a characteristic scale $R = 20$ kpc, solar position DM density $\rho(r_\odot) \equiv 0.4$ GeV/cm$^3$, and $r_\odot = 8.5$ kpc throughout this study. Second, we consider the Einasto profile,

$$\rho_{\rm Ein}(r) = \rho_\odot\ \exp\left[-\frac{2}{\alpha}\left(\left(\frac{r}{R}\right)^\alpha - 1\right)\right], \tag{6}$$

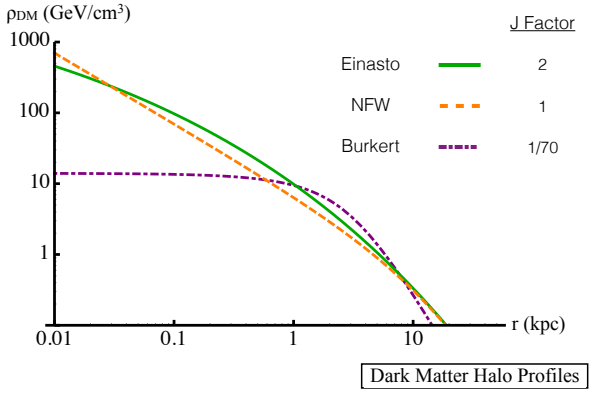


Figure 4. Dark matter galactic halo profiles, including standard Einasto and NFW profiles along with a Burkert profile with a 3 kpc core. $J$ factors are obtained assuming a spherical DM distribution and integrating over the radius from the galactic center from $r \simeq 0.05$ to 0.15 kpc. $J$ factors are normalized so that $J(\rho_{\rm NFW}) = 1$.

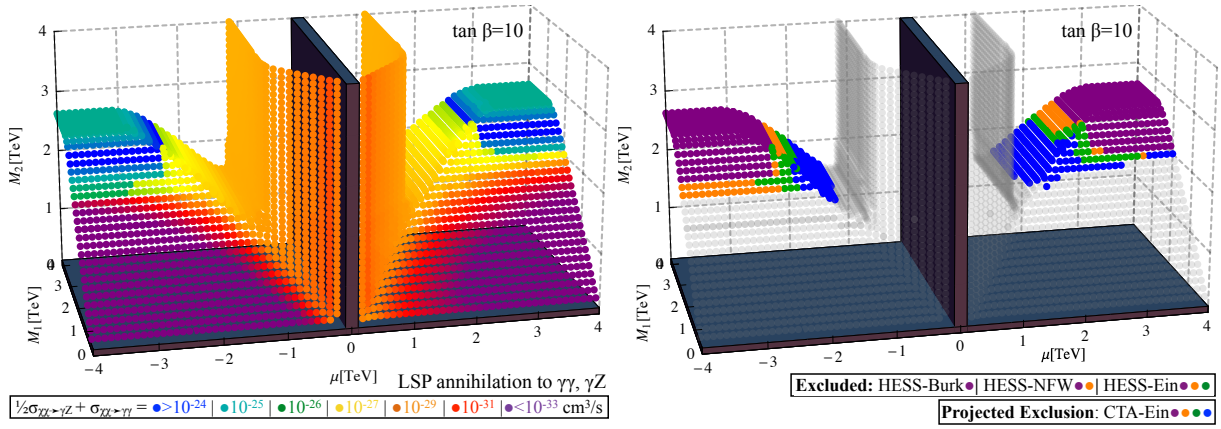


Figure 5. **Left panel:** The neutralino annihilation cross-section to $\gamma\gamma$ and $\frac{1}{2}$Z$\gamma$ is given for Milky Way velocities, as detailed in the text. **Right panel:** Relic neutralino parameters excluded by the HESS gamma ray line search, assuming Einasto, NFW, and cored (Burkert, 3 kpc) profiles, along with the projected CTA exclusion for an Einasto profile.

where we take $\alpha = 0.17$ and $R = 20$ kpc. This is the halo profile model that best fits micro-lensing and star velocity data [96, 97]. Third, we consider a Burkert or "cored" profile, with constant DM density inside radius $r_c = 3$ kpc,

$$\rho_{\rm Burk}(r) = \frac{\rho_\odot}{(1 + r/r_c)\,(1 + (r/r_c)^2)}, \tag{7}$$

For this profile, $r_c$ sets the size of the core — we assume $r_c = 3$ kpc. Assuming such a large core results in very diffuse dark matter at the galactic center, and therefore yields the weakest bound on neutralino self annihilation. On the other hand, assuming a core of smaller size (*e.g.* 0.1 kpc) only alters DM annihilation constraints by an $\mathcal{O}(1)$ factor [98].

In Figure 4, we illustrate the three halo profiles. The impact on gamma ray flux of different dark matter halo profiles is conveniently parameterized with a $J$ factor,

$$J \propto \int_{\Delta\Omega} d\Omega \int_{l.o.s.} dl\ \rho^2_{\tilde\chi}(l) \sim \int dr\ \rho^2_{\tilde\chi}(r). \tag{8}$$

We show $J$ factors integrating over the approximate H.E.S.S. galactic center gamma ray search range, $r \simeq 0.05$ to 0.15 kpc, and normalizing so that $J(\rho_{\rm NFW}) = 1$.

Galactic center gamma ray bounds on MSSM neutralinos depend on our knowledge of the cross-sections for neutralino annihilation to electroweak bosons. Neutralino annihilation rates to photons and Z bosons are known including one-loop corrections [99–102]. In addition, neutralinos annihilating non-relativistically with masses greater than $\sim$ TeV will again exhibit a Sommerfeld enhancement [56, 82, 103–111]. This can enhance pure wino annihilation to photons and weak bosons by orders of magnitude for $m_{\tilde\chi} = 1 - 5$ TeV with a typical Milky Way DM velocity $v \sim 0.001$ [112–114].

While a number of papers have addressed galactic center constraints including sommerfelded pure winos [115–117]), we provide indirect bounds on mixed neutralinos. We use the following prescription: if the neutralino LSP is more than 90% wino ($N_{12}^2 > 0.9$), we use the sommerfelded, pure wino one-loop results of Ref. [108] for $\sigma_{\tilde\chi\tilde\chi\to\gamma\gamma}$, $\sigma_{\tilde\chi\tilde\chi\to\gamma Z}$, and $\sigma_{\tilde\chi\tilde\chi\to W^+W^-}$. If the neutralino LSP is less than 90% wino we compute these cross-sections with `micrOMEGAs4` [118], which utilizes

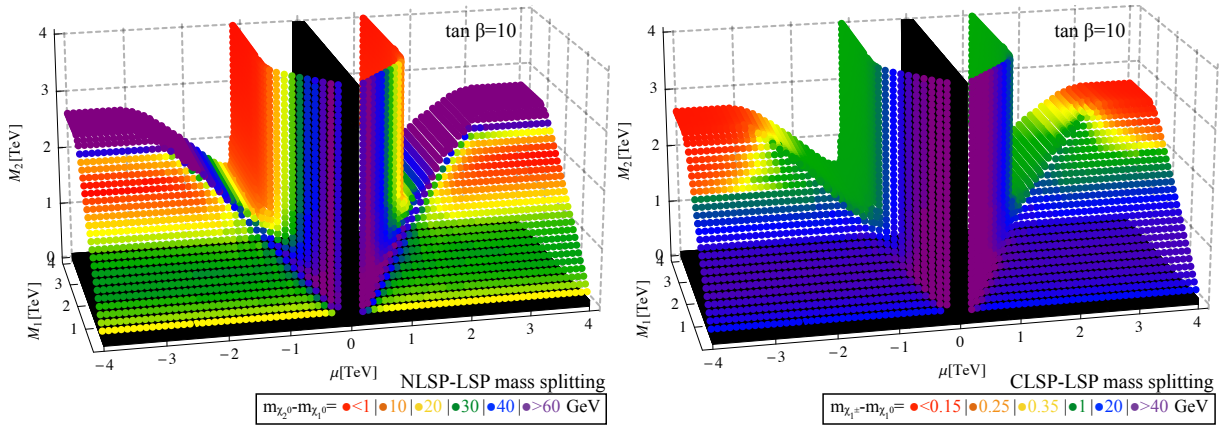


Figure 6. **Top panel:** The mass splitting between the NLSP and LSP. **Right panel:** The mass splitting between the lightest chargino (CLSP) and lightest neutralino (LSP). Parameters excluded by LEP are occluded with a black box. If the CLSP-LSP mass splitting is below roughly 1 GeV, the point is accessible with charged track searches; if CLSP-LSP and NLSP-LSP mass splittings are between 10-60 GeV, the point is accessible with compressed electroweakino searches.

one-loop results [99–102]. Because `micrOMEGAs4` does not include Sommerfeld enhancement for neutralino parameter space where ($N_{12}^2 < 0.9$), this prescription produces conservative bounds.

In Figure 5 we indicate bounds on relic neutralino dark matter from gamma ray line searches conducted by H.E.S.S. [119] along with those projected for the Cerenkov Telescope Array (CTA) [120] (see also HAWC [121]). We vary the dark matter profiles. Excluding pure wino dark using HESS and Fermi-LAT data, assuming Einasto or NFW profiles, has been studied extensively, in e.g. [115–117]. The right panel of Figure 5 shows that, for mixed electroweakinos, wino-like LSPs with a small bino or higgsinos component and mass above 2 TeV can be excluded under the assumption of an Einasto or NFW profile. However, the assumption of a more cored profile lifts bounds on some heavier relic bino-winos and wino-higgsinos. Comparing the LSP wino fraction in Figure 1 with Figure 5 shows that exclusions on relic neutralino annihilation increase with wino fraction. It is also interesting to note that, under the assumption of an Einasto profile [96, 97], CTA will probe the entire wino-higgsino surface, and all bino-winos for which the LSP is wino-like.

## V. 100 TEV COLLIDER

Because most models of dark matter are weakly-coupled to Standard Model particles, generic collider dark matter searches focus on events with large missing transverse momentum ($\not{p}_T$), arising when weakly-interacting dark matter recoils off Standard Model particles (i.e. jets, photons, leptons). On the other hand, collider searches directed at a relic, co-annihilating neutralino–chargino sector benefit from searching for electroweak radiation, emitted in inter-electroweakino decays.

For a nearly pure wino LSP, almost mass-degenerate charginos decaying to neutralinos deposit electroweak radiation as *charged tracks*. Around the wino plateau, the mass splitting between the lightest chargino and the lightest neutralino becomes compressed, as shown in Figure 6. For these points, the chargino-neutralino mass difference is set by loop effects, the chargino-neutralino decay width decreases, and the chargino lifetime is long enough for the chargino to leave noticeable paths in the detectors. Thus, typical mass splittings around 100 MeV shown in Figure 6 are ideal for disappearing charged track searches [74, 122–133].

Recently, a number of strategies for *compressed electroweakino searches* have been developed, targeting supersymmetric dark matter with $10 - 60$ GeV inter-electroweakino mass splittings [1,

130, 134–145]. These searches require a half to a fifth of the $\not{p}_T$ required by straightforward jet plus $\not{p}_T$ searches, but add the requirement of $p_T \sim 10-60$ GeV photons and leptons, which appear in the electroweakino decays.

The small mass splittings between electroweakinos, utilized by compressed and charged track searches, are a consequence of requiring that they freeze-out to the observed dark matter relic abundance with the help of co-annihilation processes. For co-annihilation to contribute significantly to the LSP annihilation, the CLSP or NLSP state must be abundant in the thermal bath when the LSP freezes out — so smaller NLSP-LSP and CLSP-LSP mass splittings increase co-annihilation. Partly because of this, nearly-pure winos, with a chargino-neutralino mass splitting of 160 MeV, are the most massive thermal relic neutralinos. In the case of bino-wino neutralinos with $M_2 < 2$ TeV, where the LSP is bino-like, the NLSP-LSP masses cannot be further apart than $m_{\tilde{\chi}_2^0} - m_{\tilde{\chi}_1^0} = 10 - 40$ GeV. Figure 6 illustrates this point, showing that precisely the regions inaccessible to direct (Figure 2), indirect (Figure 5), and present collider searches, could be tested by compressed electroweakino searches [1] at a 100 TeV proton-proton collider [146–165].

### A. Charged track search

The disappearing charged track search strategy relies on an enhanced lifetime of charginos which are around 100 MeV heavier than the dark matter agent. When the mass difference is below 1 GeV, the dominant decay mode is $\tilde{\chi}_1^\pm \to \tilde{\chi}_1^0 \pi^\pm$, which is not calculated in many of the publicly available SUSY decay codes. Using the procedure detailed in Section II we determine which points on the relic neutralino surface have a mass splitting smaller than 1 GeV and calculate their chargino-neutralino decay widths based on Ref. [166]. The resulting decay lengths range from 1-50 mm, for these points on the relic neutralino surface. Thus, even before a possible boost is taken into account, many of these charginos travel macroscopic distances before decaying. The neutralino takes the majority of the momentum of the decay products, leaving the pion with too little energy to be seen. The result is a charged track which disappears without leaving deposits of energy in the calorimeters.

To begin our study, we first calibrate our method based on the ATLAS search for disappearing tracks at 8 TeV [129]. We study a simplified model in which the chargino is 160 MeV heavier than the neutralino and has a lifetime of 0.2 ns. We generate all combinations of chargino production with up to two extra partons in the final state using `MG5aMC@NLO` [167]. These events are then showered, matched, and hadronized using `Pythia6.4` [168] with the MLM matching scheme [169]. Finally, they are passed through `DELPHES3` [170] using the default ATLAS card. Jets are defined using the anti-$k_T$ algorithm [171] with $R = 0.4$ as implemented in `FastJet` [172] and are then required to have $p_{T,j} > 20$ GeV and $|\eta_j| < 2.8$. The signal also requires a lepton veto; electron candidates are defined with $p_{T,e} > 10$ GeV and $|\eta_e| < 2.47$ while muon candidates are also defined with $p_{T,\mu} > 10$ GeV but $|\eta_\mu| < 2.4$. Following the ATLAS jet and lepton definition protocol [129], to enforce lepton isolation we remove any jet candidate within $\Delta R_{j\ell} < 0.2$ of a lepton, from jet candidates. After this, any lepton within $\Delta R = 0.4$ of remaining jet candidates is incorporated into that jet.

The final object needed for the search is the disappearing track. While `DELPHES` details charged final states with an $\eta$ and $p_T$ dependent efficiency, the charginos are not considered a final state. `Pythia` does propagate the chargino, but it does not include the effect of the magnetic field. This should have little effect as the charginos are typically boosted enough that their tracks can be reconstructed [129]. As such, we take the final location of the chargino and compute the transverse length traveled. To count as an isolated track, there must also be no jets with $p_{T,j} > 45$ GeV

within $\Delta R_{j\,\text{track}} = 0.4$. Moreover, the sum of the $p_T$ of all tracks with $p_T > 400$ MeV and within a cone of $\Delta R = 0.4$ is required to be less than 4% of the $p_T$ of the candidate isolated track. Finally, the considered chargino track must have the highest $p_T$ of all isolated tracks.

To extract the signal ATLAS then applies a series of cuts:

1. leading jet $p_{T,j} > 90$ GeV
2. missing transverse momentum $\not{p}_T > 90$ GeV
3. $\Delta\phi_{j,\not{p}_T} > 1.5$. For extra jets with $p_{T,j} > 45$ GeV this applies to the leading two jets.
4. isolated track with transverse length $= 30 - 80$ cm
5. $p_{T,\text{track}} > 15$ GeV and $0.1 < |\eta_{\text{track}}| < 1.9$.

Before applying the last cut, ATLAS provides a benchmark for a 200 GeV chargino: with 20.3 fb$^{-1}$ of integrated luminosity, they obtain 18.4 Monte Carlo events passing all other cuts. In our simulation, 23.9 events pass. We take the corresponding ratio $\epsilon_{\text{track}} = 0.77$ as a flat efficiency for measuring a disappearing track with $0.1 < |\eta| < 1.9$ and $p_T > 15$ GeV, and a track length between 30 and 80 cm. The visible cross section is then defined as

$$\sigma_{\text{vis}} = \sigma_{\text{MC}} \times \epsilon_{\text{cuts}} \times \epsilon_{\text{track}} \, . \tag{9}$$

The background for a disappearing track search is complex, because it is not dominated by a Standard Model process. Instead, it is very detector dependent and involves charged hadrons interacting with the detector material with large momentum exchange and $p_T$-mis-measured tracks. ATLAS makes a measurement of the $p_T$-mis-measured tracks and fits the shape as $d\sigma/dp_{T,\text{track}} = 1/p_{T,\text{track}}$ where $a = 1.78 \pm 0.05$. Following the example of Refs. [130] and [131], we normalize this to the total background of 18 events with $p_{T,\text{track}} > 200$ GeV with 20.3 fb$^{-1}$ of data.

Extrapolating this search to a 100 TeV collider requires some assumptions. First, since the background is detector dependent, we conservatively choose a default ATLAS setup and detector card in `DELPHES`.

We assume that the efficiency for detecting these disappearing tracks remains at a constant $\epsilon_{\text{track}} = 0.77$ across the range of parameters. Furthermore, we assume that the shape of the background remains the same at 100 TeV collisions as it was at 8 TeV. This assumption can be tested at the 13 TeV run of the LHC. The background normalization we use rescales the background found at ATLAS, by using the ratio of the $Z(\nu\bar{\nu})$+jets cross sections that pass initial analysis cuts on $p_{T,j}$, $\not{p}_T$, and $\Delta\phi_{j,\not{p}_T}$, at $\sqrt{s} = 8$ TeV and 100 TeV, respectively.

The same steps are used in Refs. [130] and [131] to estimate the background for the disappearing track signature at a 100 TeV collider. Both references acknowledge the large amount of uncertainty and present their searches for the pure wino as a band with the background 20% to 500% as large as the estimated value. Both find that a pure wino could be discovered at the 100 TeV collider, although Ref. [131] uses different cuts, resulting in improved discovery prospects. Here we combine these searches with the constrains from the observed dark matter relic abundance, including slightly mixed binos. To this end, we use the optimized cuts of Ref. [131] and scan over a representative sample of the relic neutralino surface. The optimized cuts are

$$\begin{aligned} p_{T,j_1} &> 1 \text{ TeV} & \qquad p_{T,j_2} &> 500 \text{ GeV} \\ \not{p}_T &> 1.4 \text{ TeV} & \qquad p_{T,\text{track}} &> 2.1 \text{ TeV} \, , \end{aligned} \tag{10}$$

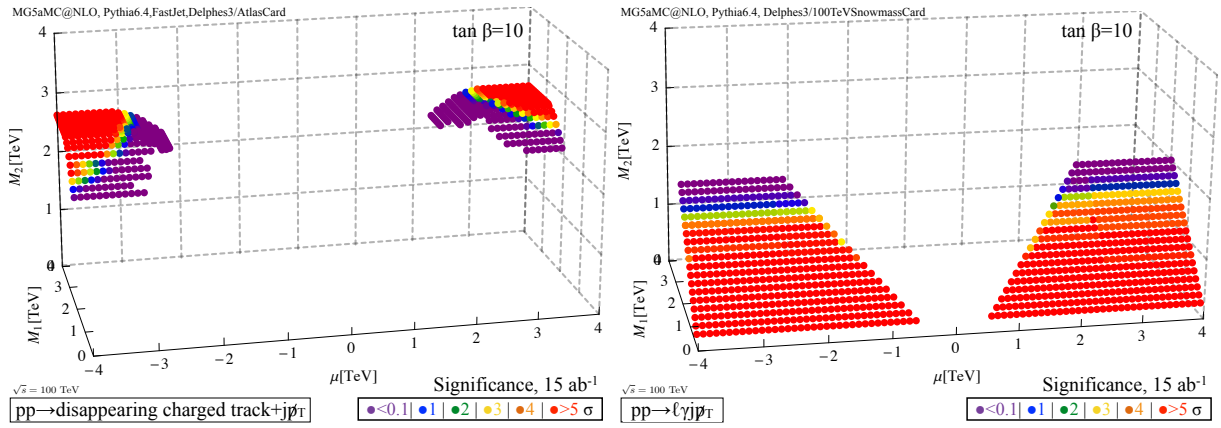


Figure 7. **Left panel:** Points on the relic neutralino surface, which will be excluded or discovered using a disappearing track search with 15 ab$^{-1}$ at a 100 TeV collider. At smaller values of $|\mu|$ the higgsino still mixes enough to cause the mass splitting of the wino plateau to be too large for the disappearing track search to be effective. **Right panel:** Points which will be excluded or discovered using a compressed search for $pp \to \ell^{\pm}\gamma j \not{p}_T$.

All other cuts are identical to the ATLAS analysis. For each of the data points we calculate the Gaussian significance

$$\#\sigma = \frac{S}{\sqrt{B + \alpha^2 B^2 + \beta^2 S^2}} \,, \tag{11}$$

where $S$ and $B$ are the number of signal and background events passing the cuts assuming 15 ab$^{-1}$ of data. The systematic uncertainties on the background and signal are conservatively given as $\alpha = 20\%$ and $\beta = 10\%$ [130, 131]. As we are scanning over a range of model parameter space with different characteristics, there is no good way to display a band of significances for the $20 - 500\%$ backgrounds. Instead, we will only quote the central background estimate. The left panel of Figure 7 shows the representative sample of points that we used mapped on the surface as well as the calculated significance. It appears that most of the wino plateau is covered and that the search works better for larger values of $|\mu|$.

For the points on the relic neutralino surface, if the decay length is less than 15 mm, the charginos have almost no chance of traveling far enough to be registered as a track. We find that for tracks longer than this, at least in the range we are considering, the points can be fit well by a cubic function. We focus on the relic neutralino points with a mass difference between the chargino and the neutralino smaller than 0.5 GeV and find their significance based on the best fit cubic curve. We then plot the points that can be discovered at $5\sigma$ and those which can be excluded at $2\sigma$. The result is shown in Figure 7. We see that most of the wino plateau is within reach, but as mixing with bino and higgsinos grows, so does the chargino-neutralino mass splitting. The chargino decay length then decreases, making the search less effective.

### B. Compressed search

Our compressed bino-wino search is directed at neutralinos with mass eigenstates separated by $1 - 40$ GeV and follows the previous study of Ref. [1]. It targets events with missing transverse momentum, photons, and leptons emitted in the decay of heavier neutralinos. The dominant

production and decay process on the relic neutralino surface is

$$pp \to (\tilde{\chi}_2^0 \to \gamma\tilde{\chi}_1^0)\,(\tilde{\chi}_1^\pm \to \ell^\pm\nu_\ell\tilde{\chi}_1^0)j \to \tilde{\chi}_1^0\tilde{\chi}_1^0\ell^\pm\nu_\ell\gamma j\;, \tag{12}$$

where the one-loop radiative decay of $\tilde{\chi}_2^0$ will be more probable as the neutralino mass splitting decreases.

As noted in the introduction to this section, for $M_2 \lesssim 2$ TeV, thermal relic neutralino mass states are arranged so that a wino-like NLSP is $10 - 40$ GeV heavier than a bino-like LSP. This electroweakino spectrum is especially amenable to searches at a 100 TeV proton-proton collider, because the lepton and photon in the dominant Standard Model background process $pp \to W^\pm\gamma j \to \nu_\ell\ell^\pm\gamma j$ tend to have higher transverse momenta whenever the final state neutrino carries enough momentum to fulfill a hard $\not{p}_T \gtrsim$ TeV requirement. The cuts we employ in this study are

$$\begin{aligned}
&p_{T,\ell} = [10-60]\text{ GeV} && |\eta_\ell| < 2.5 && \\
&p_{T,\gamma} = [10-60]\text{ GeV} && |\eta_\gamma| < 2.5 && \Delta R_{\ell\gamma} > 0.5 \\
&p_{T,j} > 0.8\text{ TeV} && |\eta_j| < 2.5 && M_{T2}^{(\gamma,\ell)} < 10\text{ GeV} \\
&\not{p}_T > 1.2\text{ TeV}\;. && && 
\end{aligned} \tag{13}$$

The cut on the lepton-photon separation, $\Delta R_{\ell\gamma}$, reduces background events in which the lepton or $W^\pm$ radiates a photon. The upper limit on the stransverse mass [173–176] of the lepton and photon, $M_{T2}^{(\gamma,\ell)}$, removes $W\gamma j$ background events: in these events the photon direction is less correlated with $\not{p}_T$ than for a decaying neutralino, $\tilde{\chi}_2^0 \to \gamma\tilde{\chi}_1^0$. We specifically use the bisection-based asymmetric $M_{T2}$ algorithm of [177]. To reject hadronic backgrounds, events with more than two jets with $p_{T,j} > 300$ GeV are vetoed. To reject electroweak backgrounds, events with more than one lepton or photon are rejected. For a lengthy discussion of this search, including the effect of background events with jets faking photons, see Ref. [1].

In the right panel of Figure 7 we show the significance attained, assuming 5% signal and background uncertainty ($\alpha = \beta = 0.05$), after 15 ab$^{-1}$ luminosity at a 100 TeV collider, obtained by simulating the signal given in Eq.(12) with the dominant $W\gamma j$ background. In this collider study, supersymmetric masses are set with `SuSpect` [73] (without loop corrections, but with inter-chargino-neutralino mass splittings manually determined using loop-level custodial symmetry breaking mass splittings, as described in Section II). The decay widths are computed with `SUSY-HIT` [178], and events are generated at tree-level in `MG5aMC@NLO` [167] and `Pythia6.4` [168]. Jets are clustered using the anti-$k_T$ algorithm [171] in `Delphes3` [170], with the Snowmass 100 TeV detector card introduced in Ref. [179].

## VI. CONCLUSIONS

We have systematically studied the phenomenology of the thermal relic neutralino dark matter surface, incorporating the effect of Sommerfeld-enhancement in setting the relic abundance at neutralino freeze-out. Spin-independent direct detection experiments will explore much of the relevant parameter space, including that of nearly-pure higgsino LSP, so long as $M_1, M_2 < 4$ TeV. Regions of nearly-pure wino LSP with will be probed by future galactic center gamma ray searches, and also with charged track searches at a future 100 TeV hadron collider. Regions with a bino-like LSP, and particularly the bino-wino space with $M_{1,2} < 2$ TeV and $|\mu| \gtrsim 1.5$ TeV can only be accessed with future compressed electroweakino searches at a 100 TeV collider (or a $\sqrt{s} \geq 4$ TeV electron-positron machine [180]). We plot $2\sigma$ exclusions of different futures experiments in Figure 8, finding a solid coverage of the sommerfelded thermal relic neutralino surface.

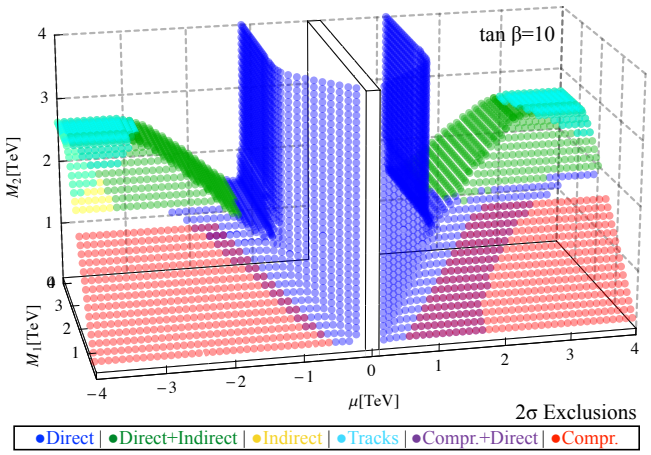


Figure 8. A combination of $2\sigma$ exclusions from future indirect (CTA and HAWC), direct (XENON1T and LZ), and collider searches (charged tracks and compressed events at 100 TeV) are shown over the surface of thermal relic neutralinos.

## ACKNOWLEDGMENTS

We thank Andrzsej Hryczuk for useful correspondence and the use of `DarkSE`. We would also like to thank Zhenyu Han and Graham Kribs for useful discussions. JB thanks CETUP for hospitality and support, as well as the Aspen Center for Physics, which is supported by National Science Foundation grant PHY-1066293. ND was partially supported by the Alexander von Humboldt Foundation. BO was partially supported by the U. S. Department of Energy under Grant Nos. DE-SC0011640. The work of AM was partially supported by the National Science Foundation under Grant No. PHY-1417118. We specifically acknowledge the assistance of the Notre Dame Center for Research Computing for computing resources.

[1] Joseph Bramante, Patrick J. Fox, Adam Martin, Bryan Ostdiek, Tilman Plehn, Torben Schell, and Michihisa Takeuchi, "Relic neutralino surface at a 100 TeV collider," Phys. Rev. **D91**, 054015 (2015), arXiv:1412.4789 [hep-ph].

[2] H. Baer, John R. Ellis, G. B. Gelmini, Dimitri V. Nanopoulos, and Xerxes Tata, "Squark Decays Into Gauginos at the $p\bar{p}$ Collider," Phys. Lett. **B161**, 175 (1985).

[3] Riccardo Barbieri, M. Frigeni, and G. F. Giudice, "Dark Matter Neutralinos in Supergravity Theories," Nucl. Phys. **B313**, 725 (1989).

[4] Manuel Drees and Mihoko M. Nojiri, "The Neutralino relic density in minimal $N = 1$ supergravity," Phys. Rev. **D47**, 376–408 (1993), arXiv:hep-ph/9207234 [hep-ph].

[5] Manuel Drees and Mihoko Nojiri, "Neutralino - nucleon scattering revisited," Phys. Rev. **D48**, 3483–3501 (1993), arXiv:hep-ph/9307208 [hep-ph].

[6] Gerard Jungman, Marc Kamionkowski, and Kim Griest, "Supersymmetric dark matter," Phys. Rept. **267**, 195–373 (1996), arXiv:hep-ph/9506380 [hep-ph].

[7] Joakim Edsjo and Paolo Gondolo, "Neutralino relic density including coannihilations," Phys.Rev. **D56**, 1879–1894 (1997), arXiv:hep-ph/9704361 [hep-ph].

[8] John R. Ellis, Toby Falk, and Keith A. Olive, "Neutralino - Stau coannihilation and the cosmological upper limit on the mass of the lightest supersymmetric particle," Phys. Lett. **B444**, 367–372 (1998), arXiv:hep-ph/9810360 [hep-ph].

[9] John R. Ellis, Toby Falk, Keith A. Olive, and Mark Srednicki, "Calculations of neutralino-stau coannihilation channels and the cosmologically relevant region of MSSM parameter space," Astropart.Phys.

**13**, 181–213 (2000), arXiv:hep-ph/9905481 [hep-ph].
[10] Jonathan L. Feng, Konstantin T. Matchev, and Frank Wilczek, "Neutralino dark matter in focus point supersymmetry," Phys. Lett. **B482**, 388–399 (2000), arXiv:hep-ph/0004043 [hep-ph].
[11] Jonathan L. Feng, Konstantin T. Matchev, and Frank Wilczek, "Prospects for indirect detection of neutralino dark matter," Phys. Rev. **D63**, 045024 (2001), arXiv:astro-ph/0008115 [astro-ph].
[12] G. J. Gounaris, C. Le Mouel, and P. I. Porfyriadis, "A description of the neutralino observables in terms of projectors," Phys. Rev. **D65**, 035002 (2002), arXiv:hep-ph/0107249 [hep-ph].
[13] Leszek Roszkowski, Roberto Ruiz de Austri, and Takeshi Nihei, "New cosmological and experimental constraints on the CMSSM," JHEP **08**, 024 (2001), arXiv:hep-ph/0106334 [hep-ph].
[14] Andreas Birkedal-Hansen and Brent D. Nelson, "The Role of Wino content in neutralino dark matter," Phys. Rev. **D64**, 015008 (2001), arXiv:hep-ph/0102075 [hep-ph].
[15] John R. Ellis, Keith A. Olive, and Yudi Santoso, "Calculations of neutralino stop coannihilation in the CMSSM," Astropart.Phys. **18**, 395–432 (2003), arXiv:hep-ph/0112113 [hep-ph].
[16] Howard Baer, Csaba Balazs, and Alexander Belyaev, "Neutralino relic density in minimal supergravity with coannihilations," JHEP **0203**, 042 (2002), arXiv:hep-ph/0202076 [hep-ph].
[17] John R. Ellis, Keith A. Olive, Yudi Santoso, and Vassilis C. Spanos, "High-energy constraints on the direct detection of MSSM neutralinos," Phys.Rev. **D69**, 015005 (2004), arXiv:hep-ph/0308075 [hep-ph].
[18] Aaron Pierce, "Dark matter in the finely tuned minimal supersymmetric standard model," Phys. Rev. **D70**, 075006 (2004), arXiv:hep-ph/0406144 [hep-ph].
[19] Takeshi Nihei and Masaki Sasagawa, "Relic density and elastic scattering cross-sections of the neutralino in the MSSM with CP violating phases," Phys.Rev. **D70**, 055011 (2004), arXiv:hep-ph/0404100 [hep-ph].
[20] Howard Baer, Azar Mustafayev, Eun-Kyung Park, and Stefano Profumo, "Mixed wino dark matter: Consequences for direct, indirect and collider detection," JHEP **07**, 046 (2005), arXiv:hep-ph/0505227 [hep-ph].
[21] Howard Baer, Tadas Krupovnickas, Azar Mustafayev, Eun-Kyung Park, Stefano Profumo, and Xerxes Tata, "Exploring the BWCA (bino-wino co-annihilation) scenario for neutralino dark matter," JHEP **12**, 011 (2005), arXiv:hep-ph/0511034 [hep-ph].
[22] N. Arkani-Hamed, A. Delgado, and G. F. Giudice, "The Well-tempered neutralino," Nucl. Phys. **B741**, 108–130 (2006), arXiv:hep-ph/0601041 [hep-ph].
[23] John R. Ellis, Keith A. Olive, and Pearl Sandick, "Phenomenology of GUT-less supersymmetry breaking," JHEP **0706**, 079 (2007), arXiv:0704.3446 [hep-ph].
[24] Carola F. Berger, James S. Gainer, JoAnne L. Hewett, and Thomas G. Rizzo, "Supersymmetry Without Prejudice," JHEP **02**, 023 (2009), arXiv:0812.0980 [hep-ph].
[25] Jonathan P. Hall and Stephen F. King, "Neutralino Dark Matter with Inert Higgsinos and Singlinos," JHEP **0908**, 088 (2009), arXiv:0905.2696 [hep-ph].
[26] Jonathan L. Feng and David Sanford, "Heart of Darkness: The Significance of the Zeptobarn Scale for Neutralino Direct Detection," JCAP **1105**, 018 (2011), arXiv:1009.3934 [hep-ph].
[27] Timothy Cohen, John Kearney, Aaron Pierce, and David Tucker-Smith, "Singlet-Doublet Dark Matter," Phys. Rev. **D85**, 075003 (2012), arXiv:1109.2604 [hep-ph].
[28] Junji Hisano, Koji Ishiwata, Natsumi Nagata, and Tomohiro Takesako, "Direct Detection of Electroweak-Interacting Dark Matter," JHEP **07**, 005 (2011), arXiv:1104.0228 [hep-ph].
[29] Maxim Perelstein and Bibhushan Shakya, "Fine-Tuning Implications of Direct Dark Matter Searches in the MSSM," JHEP **10**, 142 (2011), arXiv:1107.5048 [hep-ph].
[30] Leszek Roszkowski, Enrico Maria Sessolo, and Yue-Lin Sming Tsai, "Bayesian Implications of Current LHC Supersymmetry and Dark Matter Detection Searches for the Constrained MSSM," Phys.Rev. **D86**, 095005 (2012), arXiv:1202.1503 [hep-ph].
[31] Junji Hisano, Koji Ishiwata, and Natsumi Nagata, "Direct Search of Dark Matter in High-Scale Supersymmetry," Phys.Rev. **D87**, 035020 (2013), arXiv:1210.5985 [hep-ph].
[32] C. Strege, G. Bertone, F. Feroz, M. Fornasa, R. Ruiz de Austri, *et al.*, "Global Fits of the cMSSM and NUHM including the LHC Higgs discovery and new XENON100 constraints," JCAP **1304**, 013 (2013), arXiv:1212.2636 [hep-ph].
[33] Wolfgang Altmannshofer, Marcela Carena, Nausheen R. Shah, and Felix Yu, "Indirect Probes of the MSSM after the Higgs Discovery," JHEP **01**, 160 (2013), arXiv:1211.1976 [hep-ph].

[34] Philipp Grothaus, Manfred Lindner, and Yasutaka Takanishi, "Naturalness of Neutralino Dark Matter," JHEP **07**, 094 (2013), arXiv:1207.4434 [hep-ph].

[35] Andrew Fowlie, Malgorzata Kazana, Kamila Kowalska, Shoaib Munir, Leszek Roszkowski, *et al.*, "The CMSSM Favoring New Territories: The Impact of New LHC Limits and a 125 GeV Higgs," Phys.Rev. **D86**, 075010 (2012), arXiv:1206.0264 [hep-ph].

[36] Philip Bechtle, Torsten Bringmann, Klaus Desch, Herbi Dreiner, Matthias Hamer, *et al.*, "Constrained Supersymmetry after two years of LHC data: a global view with Fittino," JHEP **1206**, 098 (2012), arXiv:1204.4199 [hep-ph].

[37] Sophie Henrot-Versille, Remi Lafaye, Tilman Plehn, Michael Rauch, Dirk Zerwas, *et al.*, "Constraining Supersymmetry using the relic density and the Higgs boson," Phys.Rev. **D89**, 055017 (2014), arXiv:1309.6958 [hep-ph].

[38] Tao Han, Zhen Liu, and Aravind Natarajan, "Dark matter and Higgs bosons in the MSSM," JHEP **1311**, 008 (2013), arXiv:1303.3040 [hep-ph].

[39] O. Buchmueller, R. Cavanaugh, A. De Roeck, M.J. Dolan, J.R. Ellis, *et al.*, "The CMSSM and NUHM1 after LHC Run 1," Eur.Phys.J. **C74**, 2922 (2014), arXiv:1312.5250 [hep-ph].

[40] Celine Boehm, P. S. Bhupal Dev, Anupam Mazumdar, and Ernestas Pukartas, "Naturalness of Light Neutralino Dark Matter in pMSSM after LHC, XENON100 and Planck Data," JHEP **1306**, 113 (2013), arXiv:1303.5386 [hep-ph].

[41] Matthew Cahill-Rowley, JoAnne Hewett, Ahmed Ismail, and Tom Rizzo, "Constraints on Higgs Properties and SUSY Partners in the pMSSM," (2013), arXiv:1308.0297 [hep-ph].

[42] Timothy Cohen and Jay G. Wacker, "Here be Dragons: The Unexplored Continents of the CMSSM," JHEP **1309**, 061 (2013), arXiv:1305.2914 [hep-ph].

[43] Manimala Chakraborti, Utpal Chattopadhyay, Arghya Choudhury, Amitava Datta, and Sujoy Poddar, "The Electroweak Sector of the pMSSM in the Light of LHC - 8 TeV and Other Data," JHEP **1407**, 019 (2014), arXiv:1404.4841 [hep-ph].

[44] Matthew Cahill-Rowley, Randy Cotta, Alex Drlica-Wagner, Stefan Funk, JoAnne Hewett, *et al.*, "Complementarity of Dark Matter Searches in the pMSSM," (2014), arXiv:1405.6716 [hep-ph].

[45] Leszek Roszkowski, Enrico Maria Sessolo, and Andrew J. Williams, "Prospects for dark matter searches in the pMSSM," JHEP **02**, 014 (2015), arXiv:1411.5214 [hep-ph].

[46] Nishita Desai, John Ellis, Feng Luo, and Jad Marrouche, "Closing in on the Tip of the CMSSM Stau Coannihilation Strip," Phys. Rev. **D90**, 055031 (2014), arXiv:1404.5061 [hep-ph].

[47] Peisi Huang and Carlos E. M. Wagner, "Blind Spots for neutralino Dark Matter in the MSSM with an intermediate $m_A$," Phys.Rev. **D90**, 015018 (2014), arXiv:1404.0392 [hep-ph].

[48] Chris Kelso, Jason Kumar, Pearl Sandick, and Patrick Stengel, "Charged mediators in dark matter scattering with nuclei and the strangeness content of nucleons," Phys. Rev. **D91**, 055028 (2015), arXiv:1411.2634 [hep-ph].

[49] Leszek Roszkowski, Enrico Maria Sessolo, and Andrew J. Williams, "What next for the CMSSM and the NUHM: Improved prospects for superpartner and dark matter detection," JHEP **1408**, 067 (2014), arXiv:1405.4289 [hep-ph].

[50] O. Buchmueller, M. Citron, J. Ellis, S. Guha, J. Marrouche, K. A. Olive, K. de Vries, and Jiaming Zheng, "Collider Interplay for Supersymmetry, Higgs and Dark Matter," Eur. Phys. J. **C75**, 469 (2015), arXiv:1505.04702 [hep-ph].

[51] Mark D. Goodsell, Manuel E. Krauss, Tobias Mller, Werner Porod, and Florian Staub, "Dark matter scenarios in a UV-complete model with Dirac gauginos," (2015), arXiv:1507.01010 [hep-ph].

[52] Junji Hisano, Koji Ishiwata, and Natsumi Nagata, "QCD Effects on Direct Detection of Wino Dark Matter," JHEP **06**, 097 (2015), arXiv:1504.00915 [hep-ph].

[53] Timothy Cohen, Daniel J. Phalen, and Aaron Pierce, "On the Correlation Between the Spin-Independent and Spin-Dependent Direct Detection of Dark Matter," Phys. Rev. **D81**, 116001 (2010), arXiv:1001.3408 [hep-ph].

[54] Clifford Cheung, Lawrence J. Hall, David Pinner, and Joshua T. Ruderman, "Prospects and Blind Spots for Neutralino Dark Matter," JHEP **05**, 100 (2013), arXiv:1211.4873 [hep-ph].

[55] Marcin Badziak, Antonio Delgado, Marek Olechowski, Stefan Pokorski, and Kazuki Sakurai, "Detecting underabundant neutralinos," (2015), arXiv:1506.07177 [hep-ph].

[56] Junji Hisano, Shigeki Matsumoto, Minoru Nagai, Osamu Saito, and Masato Senami, "Non-perturbative effect on thermal relic abundance of dark matter," Phys. Lett. **B646**, 34–38 (2007),

arXiv:hep-ph/0610249 [hep-ph].
[57] Arnold Sommerfeld, "Uber die Beugung und Bremsung der Elektronen," Annalen der Physik **403**, 257–384 (1931).
[58] James D. Wells, "Implications of supersymmetry breaking with a little hierarchy between gauginos and scalars," (2003), arXiv:hep-ph/0306127 [hep-ph].
[59] Nima Arkani-Hamed and Savas Dimopoulos, "Supersymmetric unification without low energy supersymmetry and signatures for fine-tuning at the LHC," JHEP **0506**, 073 (2005), arXiv:hep-th/0405159 [hep-th].
[60] G.F. Giudice and A. Romanino, "Split supersymmetry," Nucl.Phys. **B699**, 65–89 (2004), arXiv:hep-ph/0406088 [hep-ph].
[61] James D. Wells, "PeV-scale supersymmetry," Phys.Rev. **D71**, 015013 (2005), arXiv:hep-ph/0411041 [hep-ph].
[62] W. Kilian, T. Plehn, P. Richardson, and E. Schmidt, "Split supersymmetry at colliders," Eur.Phys.J. **C39**, 229–243 (2005), arXiv:hep-ph/0408088 [hep-ph].
[63] Raman Sundrum, "SUSY Splits, But Then Returns," JHEP **01**, 062 (2011), arXiv:0909.5430 [hep-th].
[64] Asimina Arvanitaki, Nathaniel Craig, Savas Dimopoulos, and Giovanni Villadoro, "Mini-Split," JHEP **1302**, 126 (2013), arXiv:1210.0555 [hep-ph].
[65] Lawrence J. Hall, Yasunori Nomura, and Satoshi Shirai, "Spread Supersymmetry with Wino LSP: Gluino and Dark Matter Signals," JHEP **1301**, 036 (2013), arXiv:1210.2395 [hep-ph].
[66] James Unwin, "R-symmetric High Scale Supersymmetry," Phys.Rev. **D86**, 095002 (2012), arXiv:1210.4936 [hep-ph].
[67] Yonatan Kahn, Matthew McCullough, and Jesse Thaler, "Auxiliary Gauge Mediation: A New Route to Mini-Split Supersymmetry," JHEP **1311**, 161 (2013), arXiv:1308.3490 [hep-ph].
[68] Xiaochuan Lu, Hitoshi Murayama, Joshua T. Ruderman, and Kohsaku Tobioka, "A Natural Higgs Mass in Supersymmetry from Non-Decoupling Effects," Phys.Rev.Lett. **112**, 191803 (2014), arXiv:1308.0792 [hep-ph].
[69] Patrick J. Fox, Graham D. Kribs, and Adam Martin, "Split Dirac Supersymmetry: An Ultraviolet Completion of Higgsino Dark Matter," Phys.Rev. **D90**, 075006 (2014), arXiv:1405.3692 [hep-ph].
[70] Natsumi Nagata and Satoshi Shirai, "Higgsino Dark Matter in High-Scale Supersymmetry," (2014), arXiv:1410.4549 [hep-ph].
[71] Yasunori Nomura and Satoshi Shirai, "Supersymmetry from Typicality: TeV-Scale Gauginos and PeV-Scale Squarks and Sleptons," Phys.Rev.Lett. **113**, 111801 (2014), arXiv:1407.3785 [hep-ph].
[72] Stephen P. Martin, "A Supersymmetry primer," (1997), 10.1142/9789812839657-0001, 10.1142/9789814307505-0001, [Adv. Ser. Direct. High Energy Phys.18,1(1998)], arXiv:hep-ph/9709356 [hep-ph].
[73] Abdelhak Djouadi, Jean-Loic Kneur, and Gilbert Moultaka, "SuSpect: A Fortran code for the supersymmetric and Higgs particle spectrum in the MSSM," Comput.Phys.Commun. **176**, 426–455 (2007), arXiv:hep-ph/0211331 [hep-ph].
[74] Jonathan L. Feng, Takeo Moroi, Lisa Randall, Matthew Strassler, and Shu-fang Su, "Discovering supersymmetry at the Tevatron in wino LSP scenarios," Phys. Rev. Lett. **83**, 1731–1734 (1999), arXiv:hep-ph/9904250 [hep-ph].
[75] Tony Gherghetta, Gian F. Giudice, and James D. Wells, "Phenomenological consequences of supersymmetry with anomaly induced masses," Nucl. Phys. **B559**, 27–47 (1999), arXiv:hep-ph/9904378 [hep-ph].
[76] Masahiro Ibe, Shigeki Matsumoto, and Ryosuke Sato, "Mass Splitting between Charged and Neutral Winos at Two-Loop Level," Phys.Lett. **B721**, 252–260 (2013), arXiv:1212.5989 [hep-ph].
[77] Hsin-Chia Cheng, Bogdan A. Dobrescu, and Konstantin T. Matchev, "Generic and chiral extensions of the supersymmetric standard model," Nucl. Phys. **B543**, 47–72 (1999), arXiv:hep-ph/9811316 [hep-ph].
[78] T. Fritzsche and W. Hollik, "Complete one loop corrections to the mass spectrum of charginos and neutralinos in the MSSM," Eur.Phys.J. **C24**, 619–629 (2002), arXiv:hep-ph/0203159 [hep-ph].
[79] Marco Cirelli, Nicolao Fornengo, and Alessandro Strumia, "Minimal dark matter," Nucl. Phys. **B753**, 178–194 (2006), arXiv:hep-ph/0512090 [hep-ph].
[80] Andrzej Hryczuk and Roberto Iengo, "The one-loop and Sommerfeld electroweak corrections to the Wino dark matter annihilation," JHEP **1201**, 163 (2012), arXiv:1111.2916 [hep-ph].

[81] Andrzej Hryczuk, Ilias Cholis, Roberto Iengo, Maryam Tavakoli, and Piero Ullio, "Indirect Detection Analysis: Wino Dark Matter Case Study," JCAP **1407**, 031 (2014), arXiv:1401.6212 [astro-ph.HE].

[82] M. Beneke, C. Hellmann, and P. Ruiz-Femenia, "Non-relativistic pair annihilation of nearly mass degenerate neutralinos and charginos III. Computation of the Sommerfeld enhancements," JHEP **05**, 115 (2015), arXiv:1411.6924 [hep-ph].

[83] G. Belanger, F. Boudjema, A. Pukhov, and A. Semenov, "micrOMEGAs3: A program for calculating dark matter observables," Comput.Phys.Commun. **185**, 960–985 (2014), arXiv:1305.0237 [hep-ph].

[84] Junji Hisano, Koji Ishiwata, and Natsumi Nagata, "Gluon contribution to the dark matter direct detection," Phys. Rev. **D82**, 115007 (2010), arXiv:1007.2601 [hep-ph].

[85] Richard J. Hill and Mikhail P. Solon, "WIMP-nucleon scattering with heavy WIMP effective theory," Phys. Rev. Lett. **112**, 211602 (2014), arXiv:1309.4092 [hep-ph].

[86] Richard J. Hill and Mikhail P. Solon, "Standard Model anatomy of WIMP dark matter direct detection I: weak-scale matching," Phys. Rev. **D91**, 043504 (2015), arXiv:1401.3339 [hep-ph].

[87] Richard J. Hill and Mikhail P. Solon, "Standard Model anatomy of WIMP dark matter direct detection II: QCD analysis and hadronic matrix elements," Phys. Rev. **D91**, 043505 (2015), arXiv:1409.8290 [hep-ph].

[88] E. Aprile *et al.* (XENON100), "Dark Matter Results from 225 Live Days of XENON100 Data," Phys.Rev.Lett. **109**, 181301 (2012), arXiv:1207.5988 [astro-ph.CO].

[89] D.S. Akerib *et al.* (LUX), "First results from the LUX dark matter experiment at the Sanford Underground Research Facility," Phys.Rev.Lett. **112**, 091303 (2014), arXiv:1310.8214 [astro-ph.CO].

[90] P. Cushman *et al.*, "Working Group Report: WIMP Dark Matter Direct Detection," in *Community Summer Study 2013: Snowmass on the Mississippi (CSS2013) Minneapolis, MN, USA, July 29-August 6, 2013* (2013) arXiv:1310.8327 [hep-ex].

[91] M. Felizardo *et al.*, "Final Analysis and Results of the Phase II SIMPLE Dark Matter Search," Phys. Rev. Lett. **108**, 201302 (2012), arXiv:1106.3014 [astro-ph.CO].

[92] E. Behnke *et al.* (COUPP), "First Dark Matter Search Results from a 4-kg $CF_3I$ Bubble Chamber Operated in a Deep Underground Site," Phys. Rev. **D86**, 052001 (2012), [Erratum: Phys. Rev.D90,no.7,079902(2014)], arXiv:1204.3094 [astro-ph.CO].

[93] E. Aprile *et al.* (XENON100), "Limits on spin-dependent WIMP-nucleon cross sections from 225 live days of XENON100 data," Phys.Rev.Lett. **111**, 021301 (2013), arXiv:1301.6620 [astro-ph.CO].

[94] C. Amole *et al.* (PICO), "Dark Matter Search Results from the PICO-2L $C_3F_8$ Bubble Chamber," Phys. Rev. Lett. **114**, 231302 (2015), arXiv:1503.00008 [astro-ph.CO].

[95] Julio F. Navarro, Carlos S. Frenk, and Simon D. M. White, "The Structure of cold dark matter halos," Astrophys. J. **462**, 563–575 (1996), arXiv:astro-ph/9508025 [astro-ph].

[96] Fabio Iocco, Miguel Pato, Gianfranco Bertone, and Philippe Jetzer, "Dark Matter distribution in the Milky Way: microlensing and dynamical constraints," JCAP **1111**, 029 (2011), arXiv:1107.5810 [astro-ph.GA].

[97] Miguel Pato, Fabio Iocco, and Gianfranco Bertone, "Dynamical constraints on the dark matter distribution in the Milky Way," (2015), arXiv:1504.06324 [astro-ph.GA].

[98] Dan Hooper, Chris Kelso, and Farinaldo S. Queiroz, "Stringent and Robust Constraints on the Dark Matter Annihilation Cross Section From the Region of the Galactic Center," Astropart. Phys. **46**, 55–70 (2013), arXiv:1209.3015 [astro-ph.HE].

[99] Lars Bergstrom and Piero Ullio, "Full one loop calculation of neutralino annihilation into two photons," Nucl. Phys. **B504**, 27–44 (1997), arXiv:hep-ph/9706232 [hep-ph].

[100] Zvi Bern, Paolo Gondolo, and Maxim Perelstein, "Neutralino annihilation into two photons," Phys. Lett. **B411**, 86–96 (1997), arXiv:hep-ph/9706538 [hep-ph].

[101] Piero Ullio and Lars Bergstrom, "Neutralino annihilation into a photon and a Z boson," Phys. Rev. **D57**, 1962–1971 (1998), arXiv:hep-ph/9707333 [hep-ph].

[102] F. Boudjema, A. Semenov, and D. Temes, "Self-annihilation of the neutralino dark matter into two photons or a Z and a photon in the MSSM," Phys. Rev. **D72**, 055024 (2005), arXiv:hep-ph/0507127 [hep-ph].

[103] Junji Hisano, S. Matsumoto, and Mihoko M. Nojiri, "Unitarity and higher order corrections in neutralino dark matter annihilation into two photons," Phys. Rev. **D67**, 075014 (2003), arXiv:hep-ph/0212022 [hep-ph].

[104] Junji Hisano, Shigeki Matsumoto, and Mihoko M. Nojiri, "Explosive dark matter annihilation," Phys. Rev. Lett. **92**, 031303 (2004), arXiv:hep-ph/0307216 [hep-ph].

[105] Junji Hisano, Shigeki. Matsumoto, Mihoko M. Nojiri, and Osamu Saito, "Non-perturbative effect on dark matter annihilation and gamma ray signature from galactic center," Phys. Rev. **D71**, 063528 (2005), arXiv:hep-ph/0412403 [hep-ph].

[106] Tracy R. Slatyer, "The Sommerfeld enhancement for dark matter with an excited state," JCAP **1002**, 028 (2010), arXiv:0910.5713 [hep-ph].

[107] Andrzej Hryczuk, Roberto Iengo, and Piero Ullio, "Relic densities including Sommerfeld enhancements in the MSSM," JHEP **03**, 069 (2011), arXiv:1010.2172 [hep-ph].

[108] Andrzej Hryczuk, "The Sommerfeld enhancement for scalar particles and application to sfermion co-annihilation regions," Phys. Lett. **B699**, 271–275 (2011), arXiv:1102.4295 [hep-ph].

[109] M. Beneke, C. Hellmann, and P. Ruiz-Femenia, "Non-relativistic pair annihilation of nearly mass degenerate neutralinos and charginos I. General framework and S-wave annihilation," JHEP **03**, 148 (2013), [Erratum: JHEP10,224(2013)], arXiv:1210.7928 [hep-ph].

[110] C. Hellmann and P. Ruiz-Femena, "Non-relativistic pair annihilation of nearly mass degenerate neutralinos and charginos II. P-wave and next-to-next-to-leading order S-wave coefficients," JHEP **08**, 084 (2013), arXiv:1303.0200 [hep-ph].

[111] M. Beneke, Charlotte Hellmann, and P. Ruiz-Femenia, "Heavy neutralino relic abundance with Sommerfeld enhancements - a study of pMSSM scenarios," JHEP **03**, 162 (2015), arXiv:1411.6930 [hep-ph].

[112] Grigory Ovanesyan, Tracy R. Slatyer, and Iain W. Stewart, "Heavy Dark Matter Annihilation from Effective Field Theory," Phys. Rev. Lett. **114**, 211302 (2015), arXiv:1409.8294 [hep-ph].

[113] Matthew Baumgart, Ira Z. Rothstein, and Varun Vaidya, "Calculating the Annihilation Rate of Weakly Interacting Massive Particles," Phys. Rev. Lett. **114**, 211301 (2015), arXiv:1409.4415 [hep-ph].

[114] Martin Bauer, Timothy Cohen, Richard J. Hill, and Mikhail P. Solon, "Soft Collinear Effective Theory for Heavy WIMP Annihilation," JHEP **01**, 099 (2015), arXiv:1409.7392 [hep-ph].

[115] Timothy Cohen, Mariangela Lisanti, Aaron Pierce, and Tracy R. Slatyer, "Wino Dark Matter Under Siege," JCAP **1310**, 061 (2013), arXiv:1307.4082.

[116] JiJi Fan and Matthew Reece, "In Wino Veritas? Indirect Searches Shed Light on Neutralino Dark Matter," JHEP **10**, 124 (2013), arXiv:1307.4400 [hep-ph].

[117] Matthew Baumgart, Ira Z. Rothstein, and Varun Vaidya, "Constraints on Galactic Wino Densities from Gamma Ray Lines," JHEP **04**, 106 (2015), arXiv:1412.8698 [hep-ph].

[118] G. Blanger, F. Boudjema, A. Pukhov, and A. Semenov, "micrOMEGAs4.1: two dark matter candidates," Comput. Phys. Commun. **192**, 322–329 (2015), arXiv:1407.6129 [hep-ph].

[119] A. Abramowski *et al.* (HESS), "Search for Photon-Linelike Signatures from Dark Matter Annihilations with H.E.S.S." Phys. Rev. Lett. **110**, 041301 (2013), arXiv:1301.1173 [astro-ph.HE].

[120] Lars Bergstrom, Gianfranco Bertone, Jan Conrad, Christian Farnier, and Christoph Weniger, "Investigating Gamma-Ray Lines from Dark Matter with Future Observatories," JCAP **1211**, 025 (2012), arXiv:1207.6773 [hep-ph].

[121] A. U. Abeysekara *et al.* (HAWC), "Sensitivity of HAWC to high-mass dark matter annihilations," Phys. Rev. **D90**, 122002 (2014), arXiv:1405.1730 [astro-ph.HE].

[122] John F. Gunion and Stephen Mrenna, "A Study of SUSY signatures at the Tevatron in models with near mass degeneracy of the lightest chargino and neutralino," Phys. Rev. **D62**, 015002 (2000), arXiv:hep-ph/9906270 [hep-ph].

[123] P. Abreu *et al.* (DELPHI), "Search for charginos nearly mass - degenerate with the lightest neutralino," Eur. Phys. J. **C11**, 1–17 (1999), arXiv:hep-ex/9903071 [hep-ex].

[124] M. Acciarri *et al.* (L3), "Search for charginos with a small mass difference with the lightest supersymmetric particle at $\sqrt{S} = 189$-GeV," Phys. Lett. **B482**, 31–42 (2000), arXiv:hep-ex/0002043 [hep-ex].

[125] G. Abbiendi *et al.* (OPAL), "Search for nearly mass degenerate charginos and neutralinos at LEP," Eur. Phys. J. **C29**, 479–489 (2003), arXiv:hep-ex/0210043 [hep-ex].

[126] M. Ibe, Takeo Moroi, and T. T. Yanagida, "Possible Signals of Wino LSP at the Large Hadron Collider," Phys. Lett. **B644**, 355–360 (2007), arXiv:hep-ph/0610277 [hep-ph].

[127] Shoji Asai, Takeo Moroi, and T. T. Yanagida, "Test of Anomaly Mediation at the LHC," Phys. Lett. **B664**, 185–189 (2008), arXiv:0802.3725 [hep-ph].

[128] Matthew R. Buckley, Lisa Randall, and Brian Shuve, "LHC Searches for Non-Chiral Weakly Charged Multiplets," JHEP **05**, 097 (2011), arXiv:0909.4549 [hep-ph].

[129] Georges Aad *et al.* (ATLAS), "Search for charginos nearly mass degenerate with the lightest neutralino based on a disappearing-track signature in pp collisions at $\sqrt{(}s)$=8??TeV with the ATLAS detector," Phys.Rev. **D88**, 112006 (2013), arXiv:1310.3675 [hep-ex].

[130] Matthew Low and Lian-Tao Wang, "Neutralino dark matter at 14 TeV and 100 TeV," JHEP **08**, 161 (2014), arXiv:1404.0682 [hep-ph].

[131] Marco Cirelli, Filippo Sala, and Marco Taoso, "Wino-like Minimal Dark Matter and future colliders," (2014), arXiv:1407.7058 [hep-ph].

[132] V. Khachatryan *et al.* (CMS), "Search for disappearing tracks in proton-proton collisions at $\sqrt{s} = 8$ TeV," JHEP **01**, 096 (2015), arXiv:1411.6006 [hep-ex].

[133] Bryan Ostdiek, "Constraining the minimal dark matter fiveplet with LHC searches," Phys. Rev. **D92**, 055008 (2015), arXiv:1506.03445 [hep-ph].

[134] Pedro Schwaller and Jose Zurita, "Compressed electroweakino spectra at the LHC," JHEP **1403**, 060 (2014), arXiv:1312.7350 [hep-ph].

[135] Zhenyu Han, Graham D. Kribs, Adam Martin, and Arjun Menon, "Hunting Quasi-Degenerate Higgsinos," Phys.Rev. **D89**, 075007 (2014), arXiv:1401.1235 [hep-ph].

[136] Joseph Bramante, Antonio Delgado, Fatemeh Elahi, Adam Martin, and Bryan Ostdiek, "Catching sparks from well-forged neutralinos," Phys.Rev. **D90**, 095008 (2014), arXiv:1408.6530 [hep-ph].

[137] Chengcheng Han, Lei Wu, Jin Min Yang, Mengchao Zhang, and Yang Zhang, "New approach for detecting a compressed bino/wino at the LHC," Phys. Rev. **D91**, 055030 (2015), arXiv:1409.4533 [hep-ph].

[138] Howard Baer, Azar Mustafayev, and Xerxes Tata, "Monojet plus soft dilepton signal from light higgsino pair production at LHC14," (2014), arXiv:1409.7058 [hep-ph].

[139] Chengcheng Han, Doyoun Kim, Shoaib Munir, and Myeonghun Park, "Accessing the core of naturalness, nearly degenerate higgsinos, at the LHC," JHEP **04**, 132 (2015), arXiv:1502.03734 [hep-ph].

[140] Chengcheng Han and Myeonghun Park, "Revealing the jet substructure in a compressed spectrum," (2015), arXiv:1507.07729 [hep-ph].

[141] Nabanita Bhattacharyya and Amitava Datta, "Tracking down the elusive charginos / neutralinos through tau leptons at the Large Hadron Collider," Phys.Rev. **D80**, 055016 (2009), arXiv:0906.1460 [hep-ph].

[142] Gian F. Giudice, Tao Han, Kai Wang, and Lian-Tao Wang, "Nearly Degenerate Gauginos and Dark Matter at the LHC," Phys.Rev. **D81**, 115011 (2010), arXiv:1004.4902 [hep-ph].

[143] Lorenzo Calibbi, Jonas M. Lindert, Toshihiko Ota, and Yasutaka Takanishi, "Cornering light Neutralino Dark Matter at the LHC," JHEP **1310**, 132 (2013), arXiv:1307.4119.

[144] Stefania Gori, Sunghoon Jung, Lian-Tao Wang, and James D. Wells, "Prospects for Electroweakino Discovery at a 100 TeV Hadron Collider," (2014), arXiv:1410.6287 [hep-ph].

[145] Manimala Chakraborti, Utpal Chattopadhyay, Arghya Choudhury, Amitava Datta, and Sujoy Poddar, "Reduced LHC constraints for higgsino-like heavier electroweakinos," (2015), arXiv:1507.01395 [hep-ph].

[146] Felix Yu, "Di-jet resonances at future hadron colliders: A Snowmass whitepaper," (2013), arXiv:1308.1077 [hep-ph].

[147] Jacob Anderson, "Excited quark production at a 100 TeV VLHC," (2013), arXiv:1309.0845 [hep-ex].

[148] Timothy Cohen, Tobias Golling, Mike Hance, Anna Henrichs, Kiel Howe, *et al.*, "SUSY Simplified Models at 14, 33, and 100 TeV Proton Colliders," JHEP **1404**, 117 (2014), arXiv:1311.6480 [hep-ph].

[149] David Curtin, Patrick Meade, and Chiu-Tien Yu, "Testing Electroweak Baryogenesis with Future Colliders," (2014), arXiv:1409.0005 [hep-ph].

[150] Joseph Bramante, Jason Kumar, and John Learned, "Proton annihilation at hadron colliders and Kamioka: high-energy versus high-luminosity," Phys. Rev. **D91**, 035012 (2015), arXiv:1412.2140 [hep-ph].

[151] Andrew Fowlie and Martti Raidal, "Prospects for constrained supersymmetry at $\sqrt{s} = 33\,\text{TeV}$ and $\sqrt{s} = 100\,\text{TeV}$ proton-proton super-colliders," Eur.Phys.J. **C74**, 2948 (2014), arXiv:1402.5419 [hep-ph].

[152] Thomas G. Rizzo, "Fun with New Gauge Bosons at 100 TeV," Phys.Rev. **D89**, 095022 (2014), arXiv:1403.5465 [hep-ph].

[153] Andrew J. Larkoski and Jesse Thaler, "Aspects of Jets at 100 TeV," Phys.Rev. **D90**, 034010 (2014), arXiv:1406.7011 [hep-ph].

[154] Anson Hook and Andrey Katz, "Unbroken $SU(2)$ at a 100 TeV collider," (2014), arXiv:1407.2607 [hep-ph].

[155] Alan J. Barr, Matthew J. Dolan, Christoph Englert, Danilo Enoque Ferreira de Lima, and Michael Spannowsky, "Higgs Self-Coupling Measurements at a 100 TeV Hadron Collider," JHEP **02**, 016 (2015), arXiv:1412.7154 [hep-ph].

[156] Timothy Cohen, Raffaele Tito D'Agnolo, Mike Hance, Hou Keong Lou, and Jay G. Wacker, "Boosting Stop Searches with a 100 TeV Proton Collider," (2014), arXiv:1406.4512 [hep-ph].

[157] Bobby S. Acharya, Krzysztof Bozek, Chakrit Pongkitivanichkul, and Kazuki Sakurai, "Prospects for observing charginos and neutralinos at a 100 TeV proton-proton collider," (2014), arXiv:1410.1532 [hep-ph].

[158] David Curtin, Rouven Essig, Stefania Gori, and Jessie Shelton, "Illuminating Dark Photons with High-Energy Colliders," (2014), arXiv:1412.0018 [hep-ph].

[159] Giovanni Grilli di Cortona, "Hunting electroweakinos at future hadron colliders and direct detection experiments," JHEP **05**, 035 (2015), arXiv:1412.5952 [hep-ph].

[160] Asher Berlin, Tongyan Lin, Matthew Low, and Lian-Tao Wang, "Neutralinos in Vector Boson Fusion at High Energy Colliders," Phys. Rev. **D91**, 115002 (2015), arXiv:1502.05044 [hep-ph].

[161] A. V. Kotwal, S. Chekanov, and M. Low, "Double Higgs Boson Production in the $4\tau$ Channel from Resonances in Longitudinal Vector Boson Scattering at a 100 TeV Collider," Phys. Rev. **D91**, 114018 (2015), arXiv:1504.08042 [hep-ph].

[162] Michelangelo L. Mangano, Tilman Plehn, Peter Reimitz, Torben Schell, and Hua-Sheng Shao, "Measuring the Top Yukawa Coupling at 100 TeV," (2015), arXiv:1507.08169 [hep-ph].

[163] Philip Harris, Valentin V. Khoze, Michael Spannowsky, and Ciaran Williams, "Closing up on Dark Sectors at Colliders: from 14 to 100 TeV," (2015), arXiv:1509.02904 [hep-ph].

[164] Jan Hajer, Ying-Ying Li, Tao Liu, and John F. H. Shiu, "Heavy Higgs Bosons at 14 TeV and 100 TeV," (2015), arXiv:1504.07617 [hep-ph].

[165] Sebastian A. R. Ellis and Bob Zheng, "Reaching for Squarks and Gauginos at a 100 TeV p-p Collider," (2015), arXiv:1506.02644 [hep-ph].

[166] C. H. Chen, Manuel Drees, and J. F. Gunion, "A Nonstandard string / SUSY scenario and its phenomenological implications," Phys. Rev. **D55**, 330–347 (1997), [Erratum: Phys. Rev.D60,039901(1999)], arXiv:hep-ph/9607421 [hep-ph].

[167] J. Alwall, R. Frederix, S. Frixione, V. Hirschi, F. Maltoni, O. Mattelaer, H. S. Shao, T. Stelzer, P. Torrielli, and M. Zaro, "The automated computation of tree-level and next-to-leading order differential cross sections, and their matching to parton shower simulations," JHEP **07**, 079 (2014), arXiv:1405.0301 [hep-ph].

[168] Torbjorn Sjostrand, Stephen Mrenna, and Peter Z. Skands, "PYTHIA 6.4 Physics and Manual," JHEP **0605**, 026 (2006), arXiv:hep-ph/0603175 [hep-ph].

[169] Michelangelo L. Mangano, Mauro Moretti, Fulvio Piccinini, and Michele Treccani, "Matching matrix elements and shower evolution for top-quark production in hadronic collisions," JHEP **01**, 013 (2007), arXiv:hep-ph/0611129 [hep-ph].

[170] J. de Favereau, C. Delaere, P. Demin, A. Giammanco, V. Lematre, *et al.*, "DELPHES 3, A modular framework for fast simulation of a generic collider experiment," (2013), arXiv:1307.6346 [hep-ex].

[171] Matteo Cacciari, Gavin P. Salam, and Gregory Soyez, "The Anti-k(t) jet clustering algorithm," JHEP **0804**, 063 (2008), arXiv:0802.1189 [hep-ph].

[172] Matteo Cacciari, Gavin P. Salam, and Gregory Soyez, "FastJet User Manual," Eur.Phys.J. **C72**, 1896 (2012), arXiv:1111.6097 [hep-ph].

[173] C. G. Lester and D. J. Summers, "Measuring masses of semiinvisibly decaying particles pair produced at hadron colliders," Phys. Lett. **B463**, 99–103 (1999), arXiv:hep-ph/9906349 [hep-ph].

[174] Alan Barr, Christopher Lester, and P. Stephens, "m(T2): The Truth behind the glamour," J. Phys. **G29**, 2343–2363 (2003), arXiv:hep-ph/0304226 [hep-ph].

[175] Christopher Lester and Alan Barr, "MTGEN: Mass scale measurements in pair-production at colliders," JHEP **12**, 102 (2007), arXiv:0708.1028 [hep-ph].

[176] Hsin-Chia Cheng and Zhenyu Han, "Minimal Kinematic Constraints and m(T2)," JHEP **12**, 063 (2008), arXiv:0810.5178 [hep-ph].

[177] Chrisopher G. Lester and Benjamin Nachman, "Bisection-based asymmetric $M_{T2}$ computation: a higher precision calculator than existing symmetric methods," JHEP **03**, 100 (2015), arXiv:1411.4312 [hep-ph].

[178] A. Djouadi, M. M. Muhlleitner, and M. Spira, "Decays of supersymmetric particles: The Program SUSY-HIT (SUspect-SdecaY-Hdecay-InTerface)," *Physics at LHC. Proceedings, 3rd Conference, Cracow, Poland, July 3-8, 2006*, Acta Phys. Polon. **B38**, 635–644 (2007), arXiv:hep-ph/0609292 [hep-ph].

[179] Aram Avetisyan, John M. Campbell, Timothy Cohen, Nitish Dhingra, James Hirschauer, *et al.*, "Methods and Results for Standard Model Event Generation at $\sqrt{s} = 14$ TeV, 33 TeV and 100 TeV Proton Colliders (A Snowmass Whitepaper)," (2013), arXiv:1308.1636 [hep-ex].

[180] M Aicheler, P Burrows, M Draper, T Garvey, P Lebrun, K Peach, N Phinney, H Schmickler, D Schulte, *et al.*, "A Multi-TeV Linear Collider Based on CLIC Technology," (2012), 10.5170/CERN-2012-007.